8TH LICMAS

8th Libyan International Conference on Medical, Applied, and Social Sciences

المؤتمر الدولي الليبي الثامن للعلوم الطبية والتطبيقية والانسانية

تحت شعار: التطورات التكنولوجية والاتجاهات الحديثة في التعليم

Original articles

Enhancement of Plain Carbon Steels Corrosion by Heat Treatment of the Direct Electrodeposited Ni-P-SiC Deposit

Abdulsalam H. Salamah[1], Mohammed A. Almadani[2]*, Salah A. Gnefid[3]

[1]*Department of Petroleum Engineering, Faculty of Engineering, University of Al-Zytouna, Tarhuna, Libya*
[2]*Department of Material and Corrosion Engineering, Faculty of Engineering, University of Sebha, Sebha, Libya*
[3]*Department of Mining Engineering, Faculty of Natural Resources, University of Al-Gufra, Souknah, Libya*

ARTICLE INFO

Corresponding Email. *moh.ibrahim@sebhau.edu.ly*

Received: *16-05-2024*
Accepted: *23-06-2024*
Published: *26-06-2024*

Keywords. *Plain Carbon Steels, Ni-P Electroplating, Silicon Carbides, Heat Treatment, Hardness, Erosion Corrosion.*

ABSTRACT

The current study examined the effects of heat treatment on the microhardness and wear resistance of electrodeposited Ni-P-SiC coatings, as well as the effects of SiC particle concentrations on the coating's metallic continuous phase. Direct electrodeposition onto a low alloy steel electrode (0.40 C) was used to obtain the deposits. A modified Watt bath and pure nickel anode were used, and the material was heat treated for one hour at 400 °C. Using XRD and SEM methods, the Ni-P-SiC deposit was characterized. Additionally, the deposit's microhardness was assessed using the LECO, DM-400, both before and after heat treatment, with a 50g load. The results obtained indicate that the coating's deposition on the surface of low alloy steel and its impacts on the deposit coating crystal plane may be influenced by the applied current density. The SiC dispersion slightly improved as the bath's SiC content rose. The reduction in phosphor content of the deposited Ni-P-SiC coating as a result of the SiC particles being added to the Ni-P electrodeposition bath. The XRD data showed that crystalline Ni and Ni_3P *are formed as a result of the heat treatment procedure. As the SiC content in the electrodeposition bath and heat treatment procedure rises, so does the microhardness of the Ni-P-SiC deposit. Low alloy steel's resistance to erosion corrosion can be strengthened by the Ni-P-SiC.*

Cite this article. *Salamah A, Almadani M, Gnefid S. Enhancement of Low Alloy Steels Corrosion by Heat Treatment of the Direct Electrodeposited Ni-P-SiC Deposit. Alq J Med App Sci. 2024;7(Supp2):112-123.* https://doi.org/10.54361/ajmas.2472216

INTRODUCTION

The combined benefits of appropriate hardness, strength, and ductility can be obtained by heat treating AISA 4140 plain carbon steel throughout a broad range [1].

Coating deposition can be accomplished using a variety of techniques, such as mechanical, physical, chemical, and electrochemical ones [2]. The most common method used to create Ni-P coatings is electroless deposition, which can uniformly cover samples with intricate geometry and recesses [3,4]. Because of their high level of hardness, resistance to wear and corrosion, and low friction coefficient, Ni-P alloys are now widely utilized in the automotive, aerospace, and electronic industries [5-8]. The hardness of Ni-P coatings can be increased by adding ceramic particles like silicon carbides (SiC) and applying heat treatment, however doing so can also cause the coating to become less corrosion resistant since the addition can cause microcracks and voids in the coating [9-12]. Corrosion is a material degradation process which occurs due to chemical or electrochemical action, while erosion is a mechanical wear process. When these two processes act together the conjoint action of erosion and corrosion in aqueous environments is known as erosion corrosion [13]. Microhardness is a crucial mechanical property of metal films and coatings, and it is highly influenced by the processing parameters employed in their creation [14, 15].

The aim of the present work is to study the influence of electrodeposited conditions on the distribution of SiC incorporated particles in the Ni-P metallic matrix, the effect of the heat treatment on the electrochemical behaviour of the Ni-P-SiC (at 12 wt. % P) composite coating, in this the electrodeposition of Ni-P-SiC composites were developed in a modified watt-bath (1 L) volume with the addition of sub-micro SiC particles. The effects of current density and SiC concentration on the microhardness, the compositions and the microstructure of the deposits were also examined. The goal is to produce Ni-P-SiC composite with high hardness and wear resistance (erosion corrosion resistance) of the low alloy steels.

Almadani et. al., (2024) [16], in this research, a direct plating conditions have been used to manufacture Ni-P composite coating. Measurements of the voltage during the experiments revealed that as the experiment duration increased, so did the voltage. The current densities that were averaged were 0.08A, 0.12A, and 0.05A. In every experiment, the applied current densities resulted in the deposition of Ni-P rich material; nevertheless, the average thickness of the coating increased as the applied current density increased. The thickness of the Ni-P deposit may also increase as the temperature of the electroplating path rises. The hardness data was acquired at 285.7HV and current density of 0.08A. The Ni-P deposit-coated plain carbon steel samples underwent a one-hour heat treatment at 400°C, which increased their microhardness to roughly 443.8HV. Ni-P deposits of 8 weight percent, according to XRD examination, are thought to be in an amorphous phase. After heat treatment, they crystallized into stable phases of Ni and Ni_3P deposits.

Xiuqing Fu, et. al., (2020) [17], the impact of a magnetic field on the corrosion resistance of Ni–P and Ni–P/SiC composite coatings made by traditional jet electrodeposition was examined. Energy dispersive spectroscopy (EDS), X-ray diffraction (XRD), and scanning electron microscopy (SEM) were used to investigate the composition, surface and cross-sectional morphologies, and microstructure of the composite coatings, respectively. A laser confocal microscope LEXT4100 was used to investigate the corrosion resistance. From 0.78 V (0 T) to 0.46 V (0.5 T), the Ni-P coating's corrosion potential increased, and its corrosion current density dropped from 9.56 106 A/dm^2 (0 T) to 4.31 106 A/dm^2 (0.5 T). From 0.59 V (0 T) to 0.28 V (0.5 T), the Ni-P-SiC coating's corrosion potential increased, and its corrosion current density dropped from 6.01 ~ 10^-6 A/dm^2 (0 T) to 2.90 ~ 10^-6 A/dm^2 (0.5 T).

Donya Ahmadkhaniha, et. al., (2020) [18], SiC nanoparticle-infused Ni-P coatings and composites were created by electrodeposition, X-ray diffraction (XRD) and differential scanning calorimetry (DSC) were used to examine the structural changes brought about by heat treatment. The coatings' microhardness, scratch resistance, and corrosion resistance were assessed and contrasted both before and after various heat treatments. The findings demonstrated that the SiC particle addition to the coatings did not alter the microstructure, microhardness, or electrochemical behaviour in the as-plated condition. The function of the SiC particles was revealed in conjunction with heat treatment, though. Heat-treated composite coatings at 300 °C exhibited greater microhardness and scratch resistance compared to pure Ni-P. Furthermore, heating at 400 °C reduced the scratch resistance of the Ni-P coatings. Additionally, it was determined that heating temperature-rather than heating duration-plays a major influence in the hardness and corrosion resistance of Ni-P and composite coatings. The best heat-treatment procedure was discovered to be heating at 360 °C for two hours, which gave Ni-P and its composite coating a maximum microhardness of roughly 1500 HV0.02 without compromising corrosion resistance.

D. Ahmadkhaniha, et. al., (2018) [19], in this research, Ni-P composite coatings containing nano- and sub-mircon-sized SiC have been electrodeposited. Energy dispersive X-ray spectroscopy (EDS) and X-ray diffraction (XRD) studies were used to assess the coating's composition and structure, respectively. The outcomes demonstrated that, in contrast to nanosized particles, submicron particles can be co-deposited with a larger content. In a 3.5% NaCl solution, SiC particles had no effect on the anodic polarization behaviour of Ni-P coatings. Lastly, an investigation was conducted into the impact of particles and heat-treatment on the qualities of hardness and corrosion by studying the effects of the treatment on the coatings at 400 ºC for one hour. It was discovered that, in comparison to the as-plated circumstances, the heat treatment increased the microhardness.

METHODS

Ni-P-SiC Electrode Electrodeposition

Figure 1 showing the plain carbon steel plate (cathode) before surface preparation and the stages of plain carbon steel plate preparation for Ni-P-SiC electrodeposition.

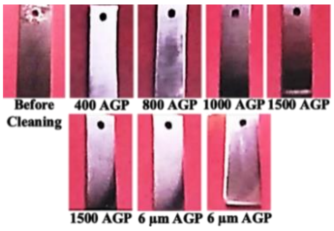

Figure 1. Low Alloy Steel (Cathodes) before Surface Preparation and the Stages of Plain Carbon Steel Plate Preparation

Ni-P-SiC Standard Substances and their Make-Up

Table 1 presenting the standard substances and their make-up of the bath used in Ni-P-SiC electrodeposition studies.

Table 1. The Standard Substances and Their Make-Up of the Bath Used in Ni-P-SiC Electrodeposition Studies.

Dissolved Substance	Chemical Formula	Purity (%)	Concentration in Bath (g/L)
Nickel Sulfate	$NiSO_4 6H_2O$	99	150
Nickel Chloride	$NiCl_2 6H_2O$	99	45
Sodium Hypophosphate	$NaH_2PO_2H_2O$	100	50
Boric Acid	H_3BO_3	99.5	50
Silicon Carbide	SiC	100	4, 5, and 6

Ni-P-SiC Electrodeposition Operating Conditions

For experiments 1.1, 2.1, 3.1, the applied current was 0.12 A, for experiments 1.2, 2.2 and 3.2, the applied current was 0.16 A and for experiments 1.3, 2.3 and 3.3 the applied current was 0.20 A. Tables 2 to 4 showed the operating conditions when the applied current density was 0.12 A, 0.16 A and 0.20 A respectively for the electrodeposition experiments.

Table 2. The Operating Conditions for Experiments 1.1, 2.1 and 3.1 at Applied Current 0.12 A.

Current Density (A/dm^2)	Bath Temperature (°C)	Bath pH	Stirring Velocity (rpm)	Anode Area (cm^2)	Anode to Cathode Distance (cm)	Experiment Duration Time (min)
2.67	65±2	2.5	150	16.2	3	240

Table 3. The Operating Conditions for Experiments 1.2, 2.2 and 3.2 at Applied Current 0.16 A.

Current Density (A/dm^2)	Bath Temperature (°C)	Bath pH	Stirring Velocity (rpm)	Anode Area (cm^2)	Anode to Cathode Distance (cm)	Experiment Duration Time (min)
3.55	65±2	2.5	150	16.2	3	180

Table 4. The Operating Conditions for Experiments 1.3, 2.3 and 3.3 at Applied Current 0.20 A.

Current Density (A/dm^2)	Bath Temperature (°C)	Bath pH	Stirring Velocity (rpm)	Anode Area (cm^2)	Anode to Cathode Distance (cm)	Experiment Duration Time (min)
4.44	65±2	2.5	150	16.2	3	120

Determination the Ni-P-SiC True Deposited Weight

Table 5 listed the calculated true weight of deposited Ni-P-SiC coating.

Determination the Average Thickness of Ni-P-SiC Deposit:

The average thickness of the deposited Ni-P-SiC coating on the surface of polished plain carbon steel plate was measured by using a microscopic technique (100x modification). Table 6 listed the thickness of the Ni-P-SiC deposit. Figure 2 showing the cross-section of Ni-P-SiC deposits under microscope (100X magnification).

Table 5. The Calculated True Weight Ni-P-SiC Deposit.

Code No.	Weight Before Electrodeposition (g)	Weight After Electrodeposition (g)	Ni-P-SiC Deposit True Weight (g)
1.1	6.9103	7.0780	0.1993
1.2	7.0602	7.3126	0.2524
1.3	7.2346	7.4172	0.1826
2.1	6.6669	6.8818	0.2149
2.2	6.6439	6.8670	0.2231
2.3	6.4798	6.6741	0.1943
3.1	6.3537	6.6210	0.2673
3.2	6.7094	6.9395	0.2301
3.3	6.7069	6.9127	0.2058

Table 6. Average Thickness of Ni-P-SiC Deposit.

Experiment Code No.	Ni-P-SiC Deposit Average Thickness (g)
1.1	37.45
1.2	56.02
1.3	40.23
2.1	41.62
2.2	41.62
2.3	40.23
3.1	58.96
3.2	43.00
3.3	45.08

Ni-P-SiC Deposit Hardness Test

The hardness tests were carried out by Vicker Hardness Tester (LECO, DM-400) with a load of (50 g). All indentations were made by applying the load (F) perpendicular to the smooth free surface of the Ni-P deposit.

Hardness Measurements Prior and After Heat Treatment

Table 7 Microhardness measurements average prior and after heat treatment process. Figure 3 showing the comparison between the microhardness measurements prior and after the heat treatment of the plain carbon steel samples coated by Ni-P deposits.

Ni-P-SiC Cross-Section and Composition Determination

The energy dispersive specimen (EDS) with a scanning electron microscope (SEM) and a Nouran instruments microanalysis system were used to assess the chemical composition of heat-treated low alloy steel specimen plates coated with Ni-P-SiC deposits.

The results of chemical composition were taken under a (SEM) at (500X) magnification. Figures 4a, 4b, 4c, 4d, 4e and 4f showing micrograph cross-section of deposits using SEM technique (500x magnification) by modified watt-bath at (2.67A/dm^2, 4 g/L), (3.55A/dm^2, 4 g/L), (2.67A/dm^2, 5 g/L), (3.55A/dm^2, 5 g/L), (2.67A/dm^2, 6 g/L), and (3.55A/dm^2, 6 g/L) respectively. Figures 5a, 5b, 5c, 5d, 5e and 5f showing micrograph cross-section of deposits using SEM technique (5000x magnification).

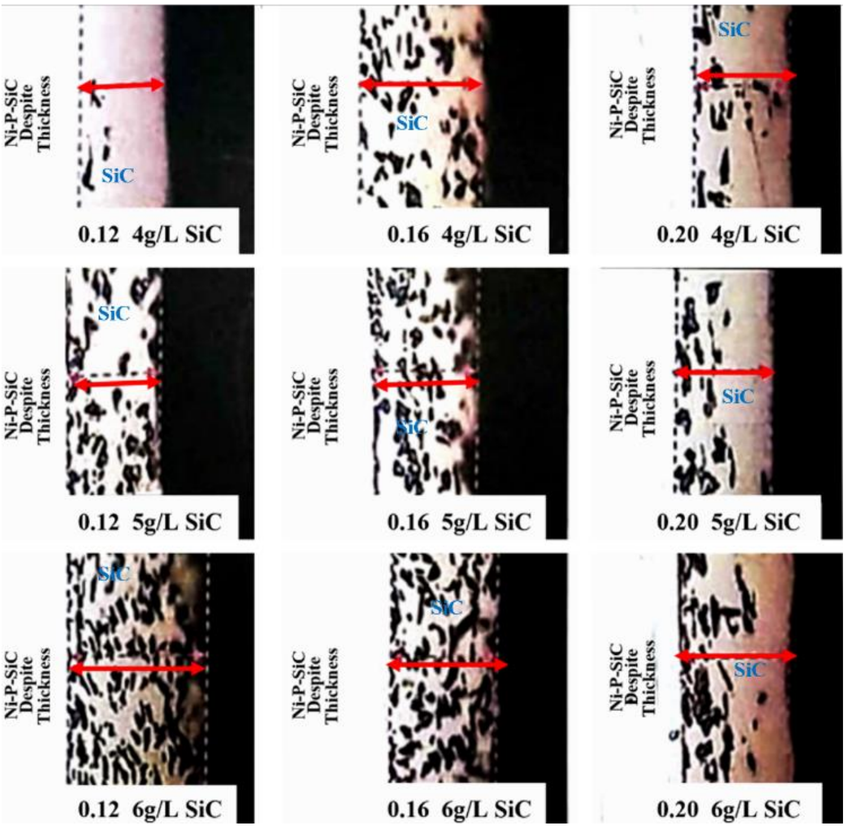

Figure 2. Ni-P-SiC Cross-section Deposits under Microscope. (100X).

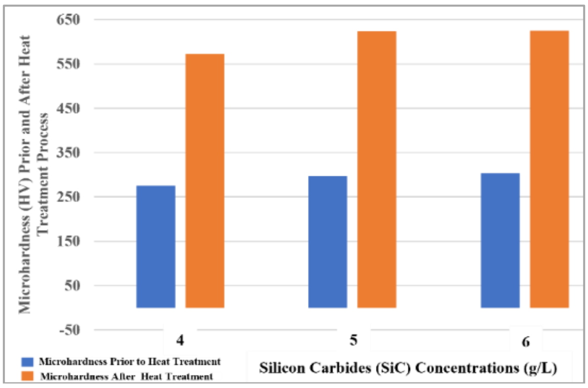

Figure 3. The comparison Between the Microhardness Measurements Prior and After the Heat Treatment of the Plain Carbon Steel Plates Coated by Ni-P-SiC Deposit.

Table 7. Microhardness Measurements Average Prior and After Heat Treatment Process.

Experiment No.	**Average Microhardness (HV)**		**Microhardness Increasing After Heat Treatment (%)**
	Prior to Heat Treatment	After Heat Treatment	
1.2	275.4	572.5	51.90
2.2	296.7	623.6	52.42
3.2	303.6	624.6	51.39
Average			51.90

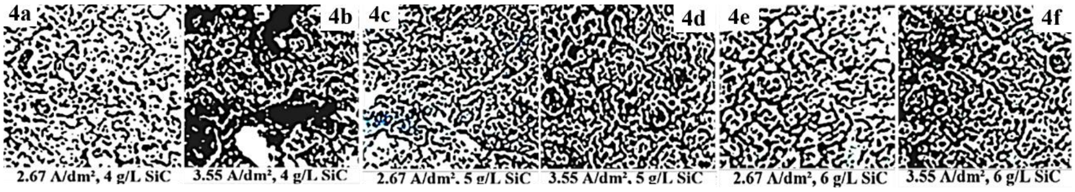

Figures 4a, 4b, 4c, 4d, 4e and 4f. (SEM) Micrograph Cross-Section (500x) of Deposits by Modified Watt-Bath at (2.67A/dm², 4 g/L), (3.55A/dm², 4 g/L), (2.67A/dm², 5 g/L), (3.55A/dm², 5 g/L), (2.67A/dm², 6 g/L), and (3.55A/dm², 6 g/L).

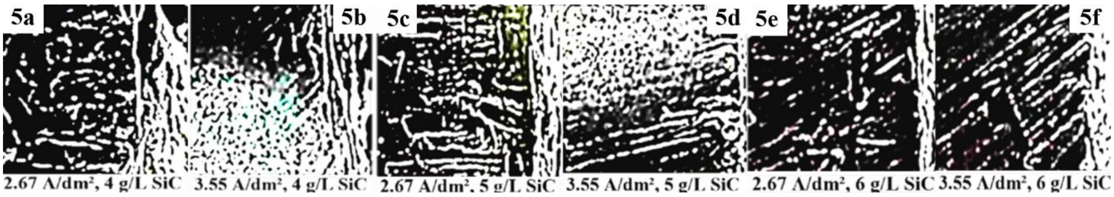

Figures 5a, 5b, 5c, 5d, 5e and 5f. (SEM) Micrograph Cross-Section (5000x) of Deposits by Modified Watt-Bath at (2.67A/dm², 4 g/L), (3.55A/dm², 4 g/L), (2.67A/dm², 5 g/L), (3.55A/dm², 5 g/L), (2.67A/dm², 6 g/L), and (3.55A/dm², 6 g/L).

Identification of Ni-P-SiC Deposits using XRD Technique

Figure 6a, 3.6b showing the XRD graphic for Ni-Pi-SiC deposit of experiment 2.2 at (3.55 A/dm², 5 g/L), 2.1 at (2.67 A/dm², 5 g/L). Figure 6b showing the identification patterns of for Ni-Pi-SiC deposit of experiment 2.2 at (3.55 A/dm², 5 g/L).

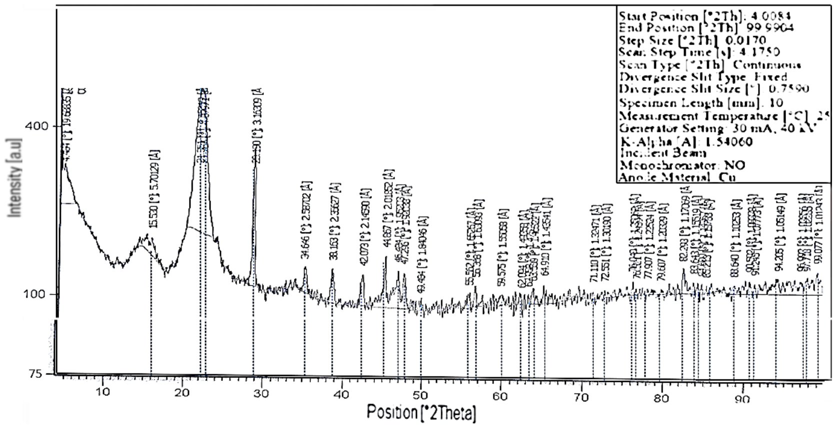

Figure 6a. XRD Graphic for Ni-Pi-SiC Deposit of Experiment 2.1 at (2.67 A/dm², 5 g/L).

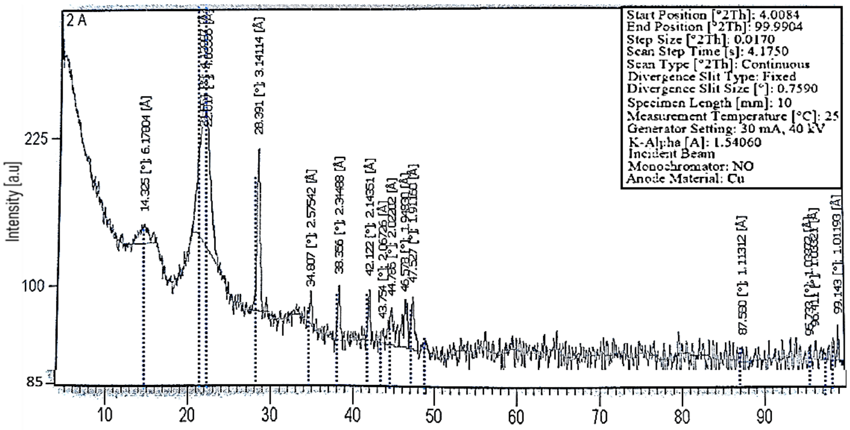

Figure 6b. XRD Graphic for Ni-Pi-SiC Deposit of Experiment 2.2 at (3.55 A/dm², 5 g/L).

Identification the Chemical Composition of AISI 4140 Plain Carbon Steel

The chemical composition of plain carbon steel was identified using (SEM) at (500X) magnification. The types of main elements and their compositions of chemical composition are listed in Table 8. Figure 7 showing the (SEM) results of the low alloy steel.

Table 8. The Chemical Composition and Elements Content of AISI 4140 Low Alloy Steel Used in the Present Work [31].

Element	Chemical Symbol	Chemical Composition Mass (%)
Carbon	C	00.40
Manganese	Mn	00.88
Chromium	Cr	00.95
Molybdenum	Mo	00.20
Iron	Fe	95.50

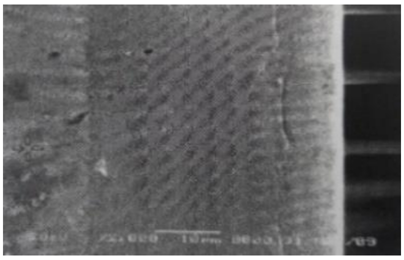

Figure 7. (SEM) Micrograph Cross-Section of AISI 4140 Plain Carbon Steel Used in the Present Work.

Erosion Corrosion Experiment of the Plain Carbon Steel

Erosion Corrosion Experiment Apparatus:

The main components of this system are: (i) 1000 Ml beaker containing hydrochloric acid (HCl 37%); (ii) Four holders partly immersed in the electrolyte; (iii) Low alloy steel plate specimens; (iv) Mechanical stirrer (stirring velocity was 150 rpm for all deposition sessions); (v) 100 g silicon carbide (SiC) particles (≈ 60 µm mesh); (vi) Steel bar holder, as shown in Figure 8.

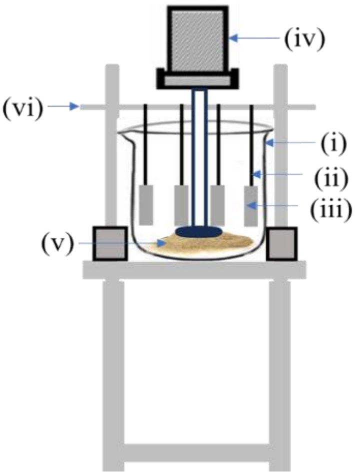

Figure 8. Apparatus of Erosion Corrosion Experiment.

The Electrolyte Preparation for Erosion Corrosion Experiment

A two mole of hydrochloric acid (HCl 37%) solution was prepared.

The Erosion Corrosion Experiment

The calculated weight loss for experiments (A) and (B) are listed in Tables 9a and 9b respectively. The low alloy steel specimens' plates electrodeposited with different concentrations of Ni-P-SiC after erosion corrosion experiments A and B are shown in Figure 9.

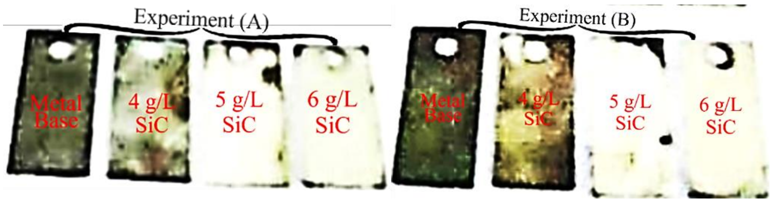

Figure 9. The Low Alloy Steel Specimens' Plates Electrodeposited with Different Concentrations of Ni-P-SiC After Erosion Corrosion Experiments A and B.

Table 9a. Data of Erosion Corrosion Experiment (A).

Specimen Code	Specimen Specification	Plate Weight Before Erosion Test (g)	Plate Weight After Erosion Test (g)	Weight Loss (g)
E1	Metal Base	5.8260	5.6138	0.2122
E2	4 g/L	5.8816	5.3645	0.5171
E3	5 g/L	5.2335	5.1078	0.1257
E4	6 g/L	5.3256	5.2333	0.0923

Table 9b. Data of Erosion Corrosion Experiment (B).

Specimen Code	Specimen Specification	Plate Weight Before Erosion Test (g)	Plate Weight After Erosion Test (g)	Weight Loss (g)
E1	Metal Base	5.8606	5.6805	0.1801
E2	4 g/L	5.6222	5.0486	0.5736
E3	5 g/L	5.2335	5.1044	0.1491
E4	6 g/L	5.2015	5.0752	0.1263

RESULTS AND DISCUSSION

Ni-P-SiC Deposit Weight and Thickness

The true weights of the Ni-P-SiC deposits obtained differ slightly, as indicated by Table's 5 results. This was attributed to the electrolyte bath, which was maintained at a constant temperature of 65±2°C throughout all experiments, while the current density varied between 2.67 A/dm², 3.55 A/dm², and 4.44 A/dm². The minimum and maximum Ni-P-SiC deposit weight were obtained at experiments 1.3 and 3.1 with 0.1826 g and 0.2673 respectively. Based on Figure 2, it is evident that the distribution of SiC particles in Ni-P varies. Applying 3.55 A/dm² to the deposit average thickness results listed in Table 6 revealed that the distribution and presence of SiC remain constant at different SiC concentrations of 4 g/L, 5 g/L, and 6 g/L. However, when the current density is increased to 4.44 A/dm², the distribution and presence of SiC in Ni-P deposit decrease at various SiC concentrations. As the bath's SiC content increased, the SiC distribution somewhat improved. It can be concluded that both the SiC content in the bath and the distribution of SiC in the Ni-P deposit of the lower applied current density 2.67 A/dm² are significant variables.

Chemical Composition of Ni-P-SiC Deposit

According to Figures 6a and 6b, the range of the phosphor contents (%) was 0.02 to 0.07, contingent upon the applied current density. As the current density rose, it decreased. This behaviour was demonstrated quite clearly when the P % decreased from 0.07 % to 0.03 % as the current density increased from 2.67 A/dm² to 3.55 A/dm². It was discovered that an additional factor contributing to the decrease in the percentage content of the deposited material was the rising SiC level in the bath. The absorption of the hydrogen ions gathered close to the cathode and stopping them from being converted to nascent hydrogen may be the cause of the decreasing P% content with increasing SiC content. Therefore, the reduction in the percentage of phosphors in the deposited Ni-P-SiC coating due to the addition of SiC particles to the Ni-P electrodeposition bath, which stops the sodium hypophosphate from being converted to phosphor [20].

XRD Analysis of Ni-P-SiC Deposits

A two-heat treated (400 °C, 1 hr) plain carbon steel specimens coated with Ni-P-SiC deposits were chosen for XRD tests to identify the microstructure of the electrodeposited coat. The XRD comparison patterns of the experiments 2.1

and 2.2 are shown in Figures 6a and 6b. According to the XRD results, it is found that the structure of Ni-P-SiC deposits were exhibiting a nickel (Ni) matrix corresponding to the matrix of the Ni-P layer in up right corner of figures under those same conditions for other phases such as Ni_3P. SiC has been found by comparing the other patterns in the figures with the XRD standard patterns [21]. It is confirmed that structural changes from amorphous state to crystalline state can be obtained in Ni-P electrodeposition coatings at 400°C. In fact, the phase of the Ni-P-SiC composite coating does not change distinctly, but after heat treatment at 400 °C for 1 hr., Ni-P-SiC leads to completely cystallization. After heat treatment, the nickel phosphide Ni_3P phase precipitates in the matrix and diffusion patterns show well-defined peaks corrosponded to crystalline Ni, Ni_3P and embeded particles shown in Figures 3.6a and 3.6b. The Ni-P-SiC deposit coating exhibits broad diffusion peaks around 2θ ranges from 04.4845° to 99.1427° for experiment 2.1 and from 14.3249° to 99.0767° for experiment 2.2. The sharp diffraction peaks at the top and wide at the bottom related to crystalline Ni and Ni_3P, they are indicating that the composite coating is composed of a mixture of crystalline and amorphous phases [22]. The crystal plane in the Ni-P-SiC deposit coating for experiment 2.1 ranges from 7.12 nm to 32.66 nm and for experiment 2.2 ranges from 13.95 nm to 43.52 nm, the average crystal plane was 21.55 nm and 27.04 for experiments 2.1 (2.67 A/dm²) and 2.2 (3.55 A/dm²) respectively. The 0.01 % increasing of the electrodeposition applied current density, causing increasing in the average crystal plane by about 20 %. The increasing in Ni-P-SiC deposit coating crystal plane of experiment 2.2 comparing to experiment 2.1 may attributed to the increasing of applied electrodeposition current density from 2.67 A/dm² to 3.55 A/dm². Slightly changes in the Ni XRD patterns recorded for coatings with same SiC content and different applied current densities of the experiments 2.1 and 2.2.

Ni-P-SiC Deposits Microhardness Prior to Heat Treatment

At current density of 3.55 A/dm², the microhardness of three plain carbon steel specimens with varying SiC concentrations of 4 g/L, 5 g/L, and 6 g/L was assessed. As indicated in Table 7 and illustrated in Figure 3, the microhardness value of the Ni-P-SiC deposit was marginally lower than that of the Ni-P containing SiC particles when no SiC particles were introduced to the electrodeposition solution. At 4 g/L of SiC, the microhardness value was 275.4 HV. However, at 5 and 6 g/L of SiC, the microhardness value increased slightly to 296.7 and 303.6 HV, the increasing of Ni-P-SiC were 7.18 % and 9.1 % respectively. The microhardness of Ni-P-SiC deposit increases with increasing the SiC content in the electrodeposition bath.

Effect of Heat Treatment on Ni-P-SiC Deposits

At current density of 3.55 A/dm², the microhardness of three plain carbon steel specimens with varying SiC concentrations of 4 g/L, 5 g/L, and 6 g/L was assessed. At 4 g/L of SiC, the microhardness value was 572.5 HV. However, at 5 and 6 g/L of SiC, the microhardness value increased slightly to 623.6 and 624.6 HV, the increasing of Ni-P-SiC were 8.19 % and 8.3 % respectively. Comparing with the microhardness values of Ni-P-SiC prior to heat treatment, for experiment 2.1 at 2.67 A/dm², the microhardness value of Ni-P-SiC deposits increased to 572.5 HV, while prior to heat treatment was 275.4 HV, the increasing in microhardness was about 52.0 %, for experiment 2.2 at 3.55 A/dm², the microhardness value of Ni-P-SiC deposits increased to 623.6 HV, while prior to heat treatment was 296.7 HV, the increasing in microhardness was also about 52.0 %, for experiment 3.3 at 4.44 A/dm², the microhardness value of Ni-P-SiC deposits increased to 624.6 HV, while prior to heat treatment was 303.6 HV, the increasing in microhardness was about 51.0 %. The creation of the intermetallic Ni_3P phase was responsible for the increase in microhardness following an hour-long heat treatment at 400°C. Hardness diminishes when coatings are heat treated beyond 400 °C due to the coarsening of Ni_3P particles and decreases in lattice defects. The precipitated Ni_3P and Ni grains are coherent with the particles as a result of heat treatment, which results in extremely high coating hardness [23]. The electrodeposited Ni-P-SiC coating on the surface of low alloy steel plates is generally heat treated at 400 °C for one hour to increase the coating's microhardness.

Effect of Erosion Corrosion on Ni-P-SiC Deposits

As shown on Figure 9, the four specimens including; metal base, three specimens electrodeposited with various SiC content; 4 g/L, 5 g/L and 6 g/L, were prepared and fixed in order to investigated the effect of commercial erodent (SiC 60 mesh) particles on the all-fixed specimen plates under the same erosion condition. The erosion test has been carried out two times under the same condition and erosion test time in order to compare the results of erosion experiments I and II. The results of weight loss of the specimens as listed in Tables 9a and 9b. Based on the eight loss results, it can be seen that in erosion corrosion experiment I, the specimen coated with Ni-P-SiC containing the higher SiC content (6 g/L) has a minimum weight loss with (0.0923 g), in this case the weight loss decreasing by 56.50 % comparing with the weight loss in the metal base. In erosion corrosion experiment I, the specimen coated with Ni-P-SiC containing the higher SiC content (6 g/L) has a minimum weight loss with (0.1263 g), in this case the weight loss decreasing by 30.00 % comparing with the weight loss in the metal base. The results for the two experiments are nearly same, and even in the Figures 9 shows that the erosion corrosion of the specimens is nearly same in the both experiments. Thus, the best erosion corrosion and wear resistance of the electrodeposition Ni-P-SiC on the surface of the low alloy steel was highly related to the concentration of the SiC content in the electrodeposition bath solution.

CONCLUSION

In the present work, a direct electrodeposition was used to create the Ni-P deposits on the surface of low alloy steel at various current densities and temperatures. The electrolyte bath used for electrodeposition was made up of boric acid, sodium hypophosphate, nickel chloride, and nickel sulphate. These approaches were effective for examining how heat treatment affected the Ni-P deposits' increased microhardness. Based on the findings, the following conclusions can be made:

(i) With the applied current density, the distribution of SiC in the Ni-P deposit and the bath's SiC content are both important variables;
(ii) The microhardness of the Ni-P-SiC deposit rises as the electrodeposition bath's SiC content does;
(iii) The microhardness of the electrodeposited Ni-P-SiC coating on the surface of AISI 4140 alloy steel plates is generally increased by heat treating it for an hour at 400 °C.
(iv) The reduction in the percentage of phosphors in the deposited Ni-P-SiC coating due to the addition of SiC particles to the Ni-P electrodeposition bath, which stops the sodium hypophosphate from being converted to phosphor.
(v) It has been established those structural transformations in Ni-P electrodeposition coatings at 400°C are possible, leading from an amorphous to a crystalline state.
(vi) The average crystal plane of the Ni-P-SiC deposit increases as the electrodeposition applied current density increases.
(vii) The wear resistance and the erosion corrosion of the Ni-P-SiC electrodeposited on the plain carbon steel and heat treated at 400 °C for 1 hr. is highly depends on the SiC contents in the electrodeposition bath solution.

Recommendations

(i) It was not looked at how current density affected Ni-P-SiC's microhardness;
(ii) To find out how particles and heat treatment affect the qualities of hardness and corrosion, it is important to examine how heat treatment affects the properties of coatings at various temperatures across various periods of time;
(iii) To look into how Ni-P-SiC electrodeposited on various AISI steel electrode types affect them in order to enhance their mechanical qualities.

REFERENCES

1. AC Manufacturing, Highest Quality Manufacturing and Machining Services, Unit 5, 10B Stadium Business Park, Ballycoolin Road, Dublin 11, D11 CKN7, Irland, 2017.
2. Sidky P & Hocking M. Review of Inorganic Coatings and Coating Processes for Reducing Wear and Corrosion. British Corrosion Journal. 1999;34(3):171–183.
3. Balaraju, J. N. & Rajam, K.S., Preparation and Characterization of Autocatalytic Low Phosphorus Nickel Coatings Containing Submicron Silicon Nitride Particles. Alloys Compound Journal, 2008; 459(1-2):311-319.
4. Mazaheri, H.; Allahkaram, S.R., Deposition, Characterization and Electrochemical Evaluation of Ni-P-Nanodiamond Composite Coatings. Appl. Surf. Sci., 2012; 258(10):4574–4580.
5. B. Łosiewicza, M. Popczykb, M. Szklarskac & P. Osakd, Effect of Phosphorus on the Corrosion Resistance of Nickel Electrocoatings, Solid State Phenomena Journal, 2015; 228: 310-316.
6. M. C. García-Alonso, V. López, M. L. Escudero & A. Macías, The Corrosion Behaviour of Laser Treated Ni/P Alloy Coatings on Mild Steel, Corrosion Science Journal,1997; 33 (4): 250–257.
7. Y.S. Huang F. Z. & Cui, Effect of Complexing Agent on the Morphology and Microstructure of Electroless Deposited Ni–P Alloy, Surface Coating Technol Journal, 2007; 201(9-11):5416-5418.
8. Shahram Alirezaei S.M., Monirvaghefi Mehdi, Salehi Mehdi & A. Saatchi, Wear Behavior of Ni–P and Ni-P-Al_2O_3 Electroless Coatings, Wear Journal, 2007; 262(7):978-985.

9. Zanella, C., Lekka, M. & Bonora, P. P., Influence of the Particle Size on the Mechanical and Electrochemical Behaviour of Micro- and Nano-Nickel Matrix Composite Coatings, Applied Electrochemistry Journal, 2009; 39(1):31-38.
10. M. Lekka, Alex Lanzutti, Caterina Zanella, Gabriel Zendron, & Lorenzo Fedrizzi, Resistance to Localized Corrosion of Pure Ni, Micro&Nano-SiC Composite Electrodeposits. Pure Applied Chemistry Journal, 2011 83(2): 295-308.
11. D. Ahmadkhaniha, F. Eriksson, P. Leisner a & C. Zanella, Effect of SiC Particle Size and Heat-Treatment on Microhardness and Corrosion Resistance of NiP Electrodeposited Coatings, Alloys Compound Journal, 2018; 769: 1080-1087.
12. Luiza Bonin, Vitry Véronique & Fabienne Delaunois, Corrosion Behaviour of Electroless High Boron-Mid Phosphorous Nickel Duplex Coatings in the as-Plated and Heat-Treated States in NaCl, H_2SO_4, NaOH and Na_2SO_4, Materials Chemistry and Physics Journal, 2018; 208:77-84.
13. Laminu Shettima Kuburi, Effect of Flow Velocity on the Inhibition Efficiency of Low Carbon Steel Corrosion in Crude Oil, Applied Mechanical Engineering Journal, 2013, 2(2): 1-4.
14. Hakamada, M., Nakamoto Y., Matsumoto, H., Iwasaki H., Chen, Y., Kusuda H. & Mabuchi M., Relationship Between Hardness and Grain Size in Electrodeposited Copper Films, Materials Science and Engineering Journal, 2007; 457(1):120-126.
15. Arun Augustin, Prashant Huilgol, K Rajendra Udupa & Udaya Bhat K, Effect of Current Density During Electrodeposition on Microstructure and Hardness of Textured Cu Coating in the Application of Antimicrobial Al Touch Surface, Mech. Behaviour Biomed. Material, 2016; 63: 352–360.
16. Mohammed A. Almadani & Salah A. Gnefid, Heat-Treated Nickel-Phosphorus Coat Deposited on the Low Alloy Steel Surface: Hardness Improvement, The Seventh Conference on Science and Technology, Sebha University, 2024.
17. Xiuqing Fu, Feixiang Wang, Xinxin Chen, Jinran Lin & Hongbing Cao, Corrosion Resistance of Ni–P/SiC and Ni–P Composite Coatings Prepared by Magnetic Field Enhanced Jet Electrodeposition, College of Engineering, The Royal Society of Chemistry Journal, 2020; 10: 34167-34176.
18. Donya Ahmadkhaniha, Fredrik Eriksson Fredrik & Zanella Caterina Zanella, Optimizing Heat Treatment for Electroplated NiP and NiP/SiC Coatings, Department of Material and Manufacturing, School of Engineering, Jönköping University, , Coatings Journal, 2018; 10(12):1179.
19. K. G. Keong, Wei Sha Wei Sha & S Malinov, Hardness Evolution of Electroless Ni-P Deposits with Thermal Processing, Metals Research Group, School of Civil Engineering, Since Direct, 2003; 168(2):263-274.
20. Brian E. Conway & Ralph E. White, Modern Aspects of Electrochemistry-No. 35, University of Ottawa, Ottawa, Ontario, Canada, Kluwer Academic Publishers- New York, eBook ISBN: 0-306-47604-5, Print ISBN: 0-306-46776-3, 2002.
21. National Bureau of Standards Monograph, Standard X-Ray Diffraction Powder Patterns, Library of Congress Catalog Card Number: 53-61386, U.S. A. Government Printing Office Washington, 1985.
22. Xiuqing Fu, Feixiang Wang, Xinxin Chen, Jinran Lin & Hongbing Cao, Corrosion Resistance of Ni-P/SiC and Ni-P Composite Coatings Prepared by Magnetic Field Enhanced Jet Electrodeposition, College of Engineering, RSC Advances Journal, 2020; 10(56):34167-34176.

تحسين تآكل الفولاذ المنخفض الكربون عن بالمعالجة الحرارية لرواسب النيكل-الفوسفو-كربيد السيليكون بالترسيب المباشر كهربائياً

عبدالسلام حسن سلامة[1]، محمد الكيلاني المدني[2]*, صالح عبدالله قنيفيد[3]

[1]قسم هندسة النفط، كلية الهندسة، جامعة الزيتونة، ترهونة، ليبيا
[2]قسم هندسة المواد والتآكل، كلية الهندسة، جامعة سبها، سبها, ليبيا
[3]قسم التعدين، كلية الموارد الطبيعية، جامعة الجفرة، سوكنة، الجفرة، ليبيا

المستخلص

تناولت الدراسة الحالية تأثيرات المعالجة الحرارية على الصلادة الدقيقة ومقاومة التآكل لطلاءات النيكل - الفوسفور - كربيد السيليكون والمترسبة كهربائياً، بالإضافة إلى تأثيرات تركيزات جسيمات كربيد السيليكون فى الطور المعدني المستمر للطلاء. تم استخدام التفريغ الكهربائي المباشر على قطب فولاذي منخفض السبائك (0.40 درجة مئوية) للحصول على الرواسب. تم استخدام حمام وات معدل وأنود النيكل النقي، وتمت معالجة المادة بالحرارة لمدة ساعة واحدة عند 400 درجة مئوية. باستخدام طرق حيود الأشعة السينية والمجهر الماسح الألكتروني، تم تقييم الصلادة الدقيقة للرواسب باستخدام جهاز الليكو، دي أم-400، قبل وبعد المعالجة الحرارية، بحمل 50 جم. تشير النتائج التي تم الحصول عليها إلى أن ترسب الطلاء على سطح الفولاذ منخفض السبائك وتأثيراته على المستوى البلوري لطلاء الرواسب قد يتأثر بكثافة التيار المطبقة. تحسن توزيع جسيمات كربيدات السلبكون قليلاً مع زيادة محتواها في محلول النيكل-فسفور في عملية الترسيب الكهربائي. أظهرت نتائج حيود الأشعة السينية أن التركيب البلوري للنيكل وفوسفايد النيكل الثلاثي يتشكلان نتيجة لإجراء المعالجة الحرارية. مع ارتفاع محتوى كربيد السيليكون وإجراءات المعالجة الحرارية، ترتفع أيضًا الصلابة الدقيقة لرواسب النيكل - الفوسفور - كربيد السيليكون. وتخلص الدراسة الى أنه يمكن تعزيز مقاومة سبائك الفولاذ المنخفض الكربون للتآكل بواسطة الترسيب الكهربائي المباشر لطلاءات النيكل - الفوسفور - كربيد السيليكون.

الكلمات المفتاحية: الفولاذ المنخفض الكربون، التكسية الكهربائية للنيكل-فسفور، كربيدات السيليكون، المعالجة الحرارية، التآكل.